Inorganic Chemistry

ARTICLE

pubs.acs.org/IC

High-Pressure Synthesis and Correlation between Structure, Magnetic, and Dielectric Properties in $LiNbO_3$-Type $MnMO_3$ (M = Ti, Sn)

Akihisa Aimi,[†] Tetsuhiro Katsumata,[‡] Daisuke Mori,[†] Desheng Fu,[§] Mitsuru Itoh,[∥] Tôru Kyômen,[⊥] Ko-ichi Hiraki,[#] Toshihiro Takahashi,[#] and Yoshiyuki Inaguma*[,†]

[†]Department of Chemistry, Faculty of Science, Gakushuin University, 1-5-1 Mejiro, Toshima-ku, Tokyo 171-8588, Japan

[‡]Department of Chemistry, Faculty of Science, Tokai University, 1117 Kitakaname, Hiratsuka, Kanagawa 259-1292, Japan

[§]Division of Global Research Leaders, Shizuoka University, Johoku 3-5-1, Naka-ku, Hamamatsu 432-8561, Japan

[∥]Materials and Structures Laboratory, Tokyo Institute of Technology, 4259 Nagatsuta, Yokohama, Kanagawa 226-8503, Japan

[⊥]Graduate School of Engineering, Department of Chemistry and Chemical Biology, Gunma University, Tenjin-cho 1-5-1, Kiryu 376-8515, Japan

[#]Department of Physics, Faculty of Science, Gakushuin University, 1-5-1 Mejiro, Toshima-ku, Tokyo 171-8588, Japan

Supporting Information

ABSTRACT: $LiNbO_3$-type $MnMO_3$ (M = Ti, Sn) were synthesized under high pressure and temperature; their structures and magnetic, dielectric, and thermal properties were investigated; and their relationships were discussed. Optical second harmonic generation and synchrotron powder X-ray diffraction measurements revealed that both of the compounds possess a polar $LiNbO_3$-type structure at room temperature. Weak ferromagnetism due to canted antiferromagnetic interaction was observed at 25 and 50 K for $MnTiO_3$ and $MnSnO_3$, respectively. Anomalies in the dielectric permittivity were observed at the weak ferromagnetic transition temperature for both the compounds, indicating the correlation between magnetic and dielectric properties. These results indicate that $LiNbO_3$-type compounds with magnetic cations are new candidates for multiferroic materials.

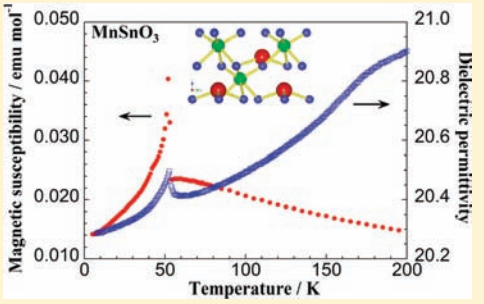

INTRODUCTION

Multiferroic materials, wherein ferroelectricity and (anti)ferromagnetism coexist, are expected in applications such as memory storage devices, sensors, actuators, and other multifunctional devices. Owing to their technological and scientific importance, much attention has been focused on multiferroic materials in general, and many investigations have been carried out on perovskite-type oxides or related oxides with 3d transition metal ions, such as $BiMO_3$ (M = Fe,[1] Mn[2]), hexagonal manganites $RMnO_3$ (R = Sc, In, Y, and Ho−Lu),[3,4] and $Pb(Fe_{2/3}W_{1/3})O_3$.[5]

Recently, we found that $LiNbO_3$-type (hereafter, abbreviated as LN-type) $ZnSnO_3$ synthesized under high pressure was polar.[6] Following this, a thin film fabricated by pulsed laser deposition was reported to exhibit ferroelectricity.[7] After these findings, we conceived that LN-type compounds with magnetic cations may be candidates of multiferroic materials. Fennie has also argued that $LiNbO_3$-type oxides with a magnetic ion such as $FeTiO_3$, $MnTiO_3$, and $NiTiO_3$ could be multiferroic candidates.[8] He also predicted that in this type of multiferroic materials, magnetism could be controlled by the electric field.

In ABO_3-type complex oxides, the LN-type structure is similar to corundum- and ilmenite-type structures in that the cations occupy two-thirds of the octahedral sites generated by the hexagonal closed packing of oxygen atoms. These structures are distinguished by the cation arrangement. In a corundum-type structure, cations are completely disordered. In an ilmenite-type structure, the cation arrangement along the *c* axis is A-B-Vac-B-A-Vac-A-... (Vac = vacancy), and the same type of cations are present in the plane perpendicular to the *c* axis. In LN-type structures, the cation arrangement along the *c* axis is A-B-Vac-A-B-Vac-A-..., and both A and B cations are included in the plane perpendicular to the *c* axis. A LN-type structure is more similar to a perovskite-type structure than a corundum-type structure in terms of the BO_6 octahedra linking at all of their corners. A LN-type structure, unlike corundum- and ilmenite-type structures, belongs to acentric crystal classes, and materials with this structure are expected to exhibit properties depending on polar structure, such as piezoelectricity, ferroelectricity, pyroelectricity, and nonlinear optical effects.[9] Although LN-type oxides would be good candidates for industrial applications, there have been few investigations into their physical properties, except for $LiNbO_3$ and $LiTaO_3$, because most LN-type oxides such as $FeMO_3$ (M = Ti,[10] Ge[11]), $MgMO_3$ (M = Ti,[12] Ge[13]), $ZnMO_3$ (M = Ge,[13] Sn[6]),

Received: May 12, 2011
Published: June 06, 2011

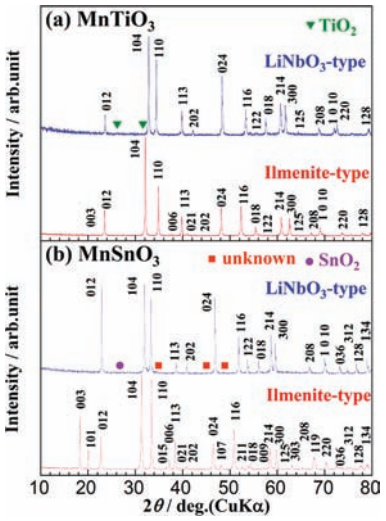

Figure 1. XRD patterns for $MnTiO_3$ (a) and $MnSnO_3$ (b). The patterns of the ilmenite-type phase (bottom of each patterns) and $LiNbO_3$-type phase (top of each patterns) are shown.

$MnMO_3$ (M = Ti,[14] Sn[15]), and $CuTaO_3$[16] are require to be synthesized under high pressures. In spite of the suitability of LN-type oxides for use as multiferroics, there are no experimental reports regarding multiferroics, except for $FeTiO_3$.[17]

In this study, we focus on LN-type $MnTiO_3$ and $MnSnO_3$ as candidates for multiferroics. Although the crystal structure and magnetic properties of $MnTiO_3$[14,18] and $MnSnO_3$[15] have been already reported, the dielectric properties and the relationship among these properties have not yet been elucidated. We synthesized these compounds and investigated their crystal structures and dielectric and magnetic properties and elucidated the correlation between these properties.

EXPERIMENTAL PROCEDURE

Ilmenite-type $MnMO_3$ (M = Ti, Sn) was synthesized as precursors for the high-pressure experiments as follows. Ilmenite-type $MnTiO_3$ was synthesized by heating an equimolar mixture of MnO and rutile-type TiO_2 in a N_2 atmosphere at 1300 °C for 5 h. Ilmenite-type $MnSnO_3$ was prepared by the ion-exchange reaction between Li_2SnO_3 and molten $MnCl_2$−KCl (molar ratio 1:3:6.09).[19] Here, Li_2SnO_3 was prepared by the solid state reaction at 800 °C for 8 h using Li_2CO_3 and SnO_2 in a molar ratio of 1.04:1 as the starting materials. LN-type $MnMO_3$ (M = Ti, Sn) was synthesized using a solid-state reaction under high pressure and high temperature using a TRY cubic multianvil-type high-pressure apparatus (NAMO 2001). Ilmenite-type $MnTiO_3$ and $MnSnO_3$ were sealed in gold capsules. A pyrophyllite cube block was used as a pressure medium. A cylindrical graphite heater was placed in the cube block. The capsules were inserted in a NaCl sleeve and placed in the heater. Then, ilmenite-type $MnTiO_3$ and $MnSnO_3$ were allowed to react at 7 GPa and 700 °C for 2 h and 800 °C for 0.5 h, respectively. After the reaction, the samples were quenched to room temperature followed by a release of pressure. As-synthesized $MnTiO_3$ and $MnSnO_3$ under high pressure were then annealed at 200 °C for 6 h in the air and 400 °C for 6 h in a N_2 atmosphere, respectively, in order to remove the internal stress brought during high-pressure synthesis. Phase identification was performed by the X-ray powder diffraction (XRD) method using a Rigaku RINT2100 diffractometer (Cu Kα radiation). Synchrotron XRD data for structural analyses were collected on a Debye−Scherrer type powder diffractometer with an imaging-plate type detector installed in beamline BL02B2 at SPring-8, Hyogo in Japan. The wavelength of the incident synchrotron radiation was fixed at 0.52035 Å. The samples were packed into a glass capillary having a diameter of 0.2 mm. The structural parameters were refined by the Rietveld analysis using the program RIETAN-FP.[20] The optical second harmonic generation (SHG) response was qualitatively tested for ungraded powders using a Continuum Minilite YAG:Nd laser (λ = 1064 nm). The magnetic properties were measured between 5 and 300 K in an applied magnetic field of up to 1 T by using a Quantum Design MPMS SQUID magnetometer. Heat capacity measurements were performed using a Quantum Design PPMS system from 2 to 100 K under zero magnetic field and a DC magnetic field of 9 T. Dielectric permittivity measurements were performed using an Agilent 4284 precision LCR meter and a Quantum design PPMS system for frequencies of 1 kHz to 1 MHz under zero magnetic field and a DC magnetic field of 9 T.

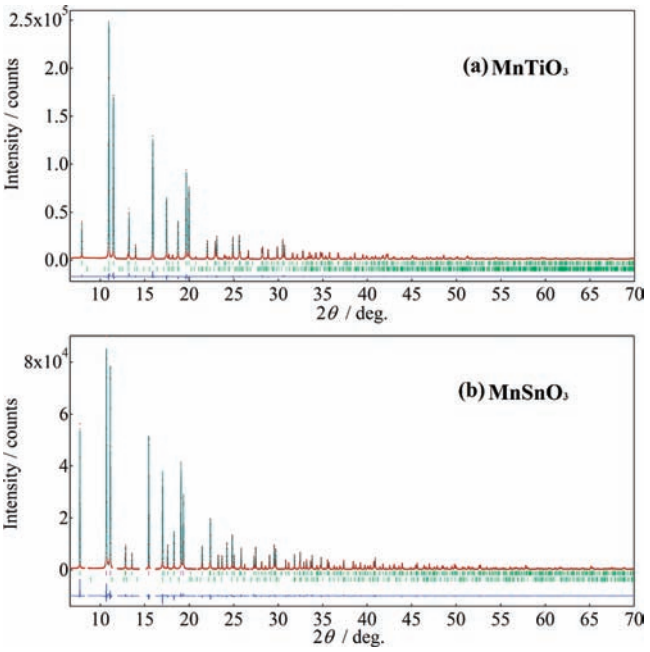

Figure 2. Observed (crosses), calculated (solid line), and difference (bottom) X-ray powder diffraction patterns for $LiNbO_3$-type $MnTiO_3$ (a) and $MnSnO_3$ (b) after refinement in space group *R*3*c*. Peak positions of $MnTiO_3$ (up) and TiO_2 (bottom) for (a) and $MnSnO_3$ (up) and SnO_2 (bottom) for (b) are indicated.

RESULTS AND DISCUSSION

A. Phase Identification, Crystal Structure, and Polarity. The XRD patterns for $MnMO_3$ (M = Ti and Sn) synthesized under high pressure are shown in Figure 1 together with those of the ilmenite-type phases. High -pressure phases of $MnMO_3$ (M = Ti, Sn) crystallize in a hexagonal structure. No change in the hexagonal phases of $MnMO_3$ (M = Ti, Sn) was observed after annealing at 200 °C for 6 h in the air and 400 °C for 6 h in a N_2 atmosphere, respectively. Small amounts of TiO_2 (high-pressure phase) for $MnTiO_3$ and SnO_2 (rutile) and unknown impurities for $MnSnO_3$ were observed. Considering the reflection conditions of the main hexagonal phases, the possible space groups were noncentrosymmetric *R*3*c* or centrosymmetric $R\bar{3}c$ for both compounds. SHG signals were observed for both compounds, indicating that $MnMO_3$ (M = Ti, Sn) is noncentrosymmetric and has the polar space group *R*3*c*, as noted previously.[18,21] The structural parameters were then refined on the basis of an LN-type structure. Figure 2a,b show the calculated, observed, and

dx.doi.org/10.1021/ic201006q |*Inorg. Chem.* 2011, 50, 6392–6398

Table 1. Structural Parameters of $MnTiO_3$[a]

atom	site	g	x	y	z	$B/Å^2$
Mn	6a	1.0	0	0	0.27602(18)	0.48(2)
Ti	6a	1.0	0	0	0	0.259(18)
O	18b	1.0	0.0600(5)	0.3420(5)	0.0641(2)	0.36(3)

[a] Hexagonal, space group $R3c$ (No. 161), $Z = 6$, $a = 5.20597(9)$ Å, $c = 13.69518(18)$ Å. $R_{wp} = 3.42\%$, $R_p = 2.48\%$, $R_e = 1.83\%$, $S = 1.86$, $R_I = 1.34\%$, $R_F = 1.06\%$.

Table 2. Structural Parameters of $MnSnO_3$[a]

atom	site	g	x	y	z	$B/Å^2$
Mn	6a	1.0	0	0	0.28145(15)	0.44(3)
Sn	6a	1.0	0	0	0	0.193(12)
O	18b	1.0	0.0517(12)	0.3545(17)	0.0699(6)	0.29(10)

[a] Hexagonal, space group $R3c$ (No. 161), $Z = 6$, $a = 5.37511(9)$ Å, $c = 14.0236(2)$ Å; $R_{wp} = 5.66\%$, $R_p = 4.04\%$, $R_e = 3.06\%$, $S = 1.85$, $R_I = 0.96\%$, $R_F = 0.45\%$.

Table 3. Selected Bond Lengths and Angles for $MnTiO_3$ and $MnSnO_3$

bond	$MnTiO_3$	$MnSnO_3$
	bond distance (Å)	
Mn−O (×3)	2.118(3)	2.111(8)
Mn−O (×3)	2.289(3)	2.342(8)
M−O (×3)	1.866(3)	2.034(7)
M−O (×3)	2.110(3)	2.100(8)
	bond angle (deg)	
Mn−O−Mn	117.8(2)	121.4(3)

difference synchrotron X-ray diffraction patterns for $MnTiO_3$ and $MnSnO_3$, respectively. The refined structures for both $MnTiO_3$ and $MnSnO_3$ are the same as that of $LiNbO_3$. The amount of impurity phases of TiO_2 in $MnTiO_3$ and SnO_2 in $MnSnO_3$ are estimated to be 0.38 mol % and 0.05 mol %, respectively. The refined structural parameters for $MnTiO_3$ and $MnSnO_3$ are listed in Tables 1 and 2, respectively. The lattice volumes of the LN-type phases, 53.6 $Å^3$/fu for $MnTiO_3$ and 58.5 $Å^3$/fu for $MnSnO_3$, are smaller than those of ilmenite-type phases, 54.5 $Å^3$/fu for $MnTiO_3$ and 60.0 $Å^3$ /fu for $MnSnO_3$, which is consistent with the fact that LN-type phases can be synthesized using the ilmenite phases under high-pressure conditions. The selected bond lengths and bond angles are listed in Table 3. The structures of $MnMO_3$ (M = Ti, Sn) in terms of the MnO_6 and MO_6 octahedra are shown in Figure 3a,b, respectively. The program VESTA[22] was used for the drawings. The calculated bond valence sum[23] (BVS), the distortion of the M-site octahedron Δ (see Figure 2b), and spontaneous polarization P are summarized in Table 4. Δ is estimated by the following equation:[24]

$$\Delta = \frac{1}{6}\sum_i \left\{\frac{(d_i - d_{ave})}{d_{ave}}\right\}^2 \quad (1)$$

where d_i and d_{ave} are the interatomic distances of M−O and its average value, respectively. P is estimated by using the structural

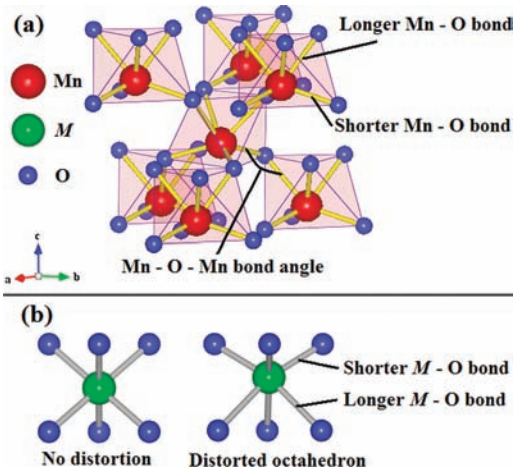

Figure 3. (a) Linkage of MnO_6 octahedra in $LiNbO_3$-type $MnMO_3$ (M = Ti, Sn). (b) MO_6 octahedron without distortion (left) and distorted by displacement of oxygen ions (right). The bond lengths and angles are summarized in Table 3.

Table 4. Bond Valence Sums, Distortion of Octahedron, and Spontaneous Polarization Derived from Structural Parameters for $MnTiO_3$ and $MnSnO_3$

	BVS			
	Mn	M	$\Delta \times 10^{-4}$	P ($\mu C/cm^2$)
$MnTiO_3$	2.02	3.98	38(1)	68.65(9)
$MnSnO_3$	1.94	3.88	2.6(9)	55.1(2)

data according to the equation

$$P = \sum_i q_i \delta z_i / V \quad (2)$$

where q_i, δz_i, and V are the formal charge of each ion, displacement of each ion along the c axis, and unit cell volume, respectively. In $MnTiO_3$, the BVSs of Mn and Ti were 2.02 and 3.98, respectively. In $MnSnO_3$, the BVSs of Mn and Sn were 1.94 and 3.88, respectively. These results indicate that the oxidation states of Mn and M were +2 and +4, respectively. Δ for $MnTiO_3$ ($\Delta = 38 \times 10^{-4}$) was more than 10 times greater than that for $MnSnO_3$ ($\Delta = 2.6 \times 10^{-4}$). The greater magnitude of Δ in $MnTiO_3$ originates from the second-order Jahn−Teller (hereafter abbreviated as SOJT) effect,[25] i.e., the mixing of the filled oxygen shell and the empty d shell of Ti^{4+} ion. The calculated spontaneous polarization of $MnTiO_3$ ($P = 69\ \mu C/cm^2$) was higher than that of $MnSnO_3$ ($P = 55\ \mu C/cm^2$), which was primarily due to the greater displacement of M in MO_6 of $MnTiO_3$ than that in $MnSnO_3$. Although $MnSnO_3$ had no SOJT active cation, this compound exhibited greater spontaneous polarization than SOJT active $BaTiO_3$ ($P = 18\ \mu C/cm^2$ and $\Delta = 29 \times 10^{-4}$).[26] This is because the contribution of the A-site cation for P is large in the $LiNbO_3$-type structure.

B. Magnetic Properties and Specific Heat of $MnTiO_3$ and $MnSnO_3$. Figure 4a shows the temperature dependences of magnetic susceptibility χ measured in an applied magnetic field of 0.01 T in both zero field cooled (ZFC) and field cooled (FC) modes for $MnTiO_3$. The effective Bohr magneton number was calculated to be 5.85 from the data obtained in the temperature range 150−290 K, which is consistent with the theoretical value

dx.doi.org/10.1021/ic201006q |Inorg. Chem. 2011, 50, 6392–6398

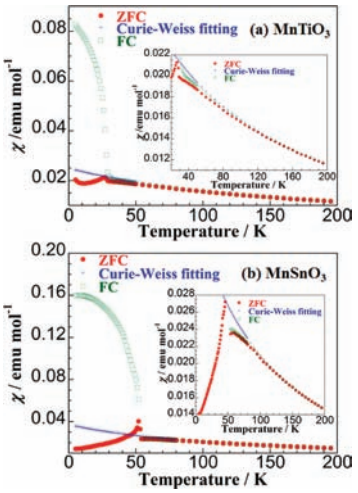

Figure 4. Temperature dependences of ZFC and FC magnetic susceptibilities at 0.01 T and Curie−Weiss fit for MnTiO (a) and $MnSnO_3$ (b). Insets show the enlarged fragment with the observed magnetic susceptibilities.

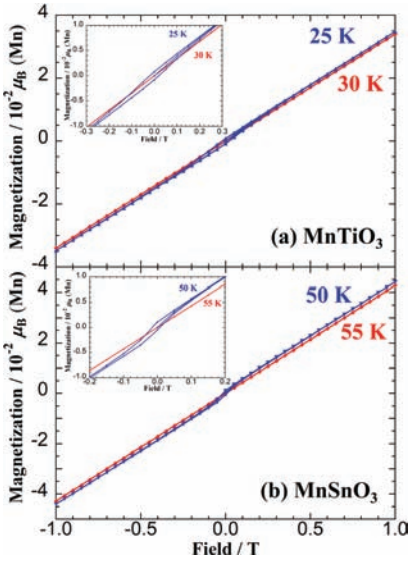

Figure 5. Isothermal magnetizations at 25 and 30 K for $MnTiO_3$ (a) and at 50 and 55 K for $MnSnO_3$ (b). Insets show the extended figures.

of 5.92 expected from Mn^{2+} (S = 5/2). The derived Weiss temperature is −176 K, indicating that the magnetic interaction is antiferromagnetic. As shown in the inset in Figure 4a, below 130 K, a deviation was observed from the Curie−Weiss law. Abrupt rises were observed around 28 K (hereafter abbreviated as T_1), which is near the Néel temperature (24 K) reported by Syono et al.,[14] in both ZFC and FC magnetic susceptibilities and in the magnetic field up to 1 T. Figure 5a shows the isothermal magnetization measured at 25 and 30 K, just below and above the abrupt rise, respectively. As shown in the inset in Figure 5a, a clear hysteresis is observed at 25 K, indicating that the abrupt rise in χ at T_1 can be assigned to the onset of weak ferromagnetism (hereafter abbreviated as T_{WFM}). The weak ferromagnetism is due to the canted antiferromagnetic interaction between the Mn ions via oxygen, i.e., a superexchange interaction. The magnetic moment was estimated to be 0.001 μ_B/Mn at 25 K. This value is lower than that of LN-type $FeTiO_3$ (0.008 μ_B/Fe) at 105 K just below T_{WFM} (110 K),[17] which is attributed to the magnitude of the spin−orbit effect.[8] The weak ferromagnetic ordering produced branching of ZFC and FC magnetic susceptibilities below T_{WFM}, as shown in Figure 4a.

Figure 4b shows the temperature dependences of magnetic susceptibility χ at 0.01 T in both ZFC and FC modes for $MnSnO_3$. The effective Bohr magneton number was calculated to be 6.20 from the data obtained in the temperature range 140−280 K, which is larger than the theoretical value. The Weiss temperature is −130 K, indicating that the magnetic interaction is antiferromagnetic. As shown in the inset in Figure 4b, below 120 K, a deviation was observed from the Curie−Weiss law. Abrupt rises in χ, as with $MnTiO_3$, were observed up to 1 T at 53 K. Though Mn_2SnO_4 is possible as a magnetic impurity phase, which undergoes a ferrimagnetic transition at 53−58 K,[27] no peak corresponding to Mn_2SnO_4 was observed in the XRD pattern for $MnSnO_3$. Therefore, in this study, the influence of this phase on magnetic properties has not been considered. In the ZFC and FC magnetic susceptibilities, branching was observed below the temperature of abrupt rise. Figure 5b shows the isothermal magnetization measured at 50 and 55 K. Similar to $MnTiO_3$, weak ferromagnetic behavior was observed just below the abrupt rise. The saturated magnetic moment was estimated to be 0.0016 μ_B/Mn.

Temperature dependences of the total specific heat (hereafter abbreviated as C) under a magnetic field of 0 and 9 T for $MnTiO_3$ and $MnSnO_3$ are shown in Figure 6a,c, respectively. Typical λ-type transitions were observed at T_{WFM} for both the compounds, indicating that the observed magnetic transitions correspond to those for the bulk materials and not to the impurity phases. The λ-type peaks shifted slightly to the high temperature side with an applied magnetic field of 9 T. The magnetic specific heat (hereafter abbreviated as C_{mag}) was estimated by subtracting the lattice specific heat from C. The lattice contribution of C was estimated by extrapolation from the data, except around the peak. The temperature dependences of the magnetic specific heat divided by temperature (hereafter abbreviated as C_{mag}/T) and the magnetic entropy (hereafter abbreviated as ΔS) are shown in Figure 6b,d for $MnTiO_3$ and $MnSnO_3$, respectively. The resulting entropy was 9.3 J mol^{-1} K^{-1} for $MnTiO_3$ and 8.7 J mol^{-1} K^{-1} for $MnSnO_3$, which are less than that expected for a Mn^{2+} ion (14.9 J mol^{-1} K^{-1}) from the following equation:

$$\Delta S = R \ln(2S + 1) \quad (3)$$

where R is the gas constant and S is the spin angular momentum quantum number. This finding suggests the presence of a short-range magnetic interaction above the transition temperature T_{WFM}, which is supported by the fact that the magnetic susceptibilities deviated from the Curie−Weiss law below 130 K, as mentioned above.

The temperature dependences of the magnetic susceptibility for both the compounds can be explained as follows. On cooling, antiferromagnetic interaction occurred, and at T_{WFM}, these compounds underwent long-range antiferromagnetic ordering with weak ferromagnetism (corresponding to the abrupt rises). This is the first observation in these compounds. The differences in the onset of antiferromagnetic ordering between $MnTiO_3$ and $MnSnO_3$ originates from the magnetic interaction between Mn ions via oxygen, i.e., the Mn−O−Mn bond angle (see Table 3). Reflecting the larger Mn−O−Mn bond angle in $MnSnO_3$ (121.4°) than that in $MnTiO_3$ (117.8°), the long-range

dx.doi.org/10.1021/ic201006q |Inorg. Chem. 2011, 50, 6392–6398

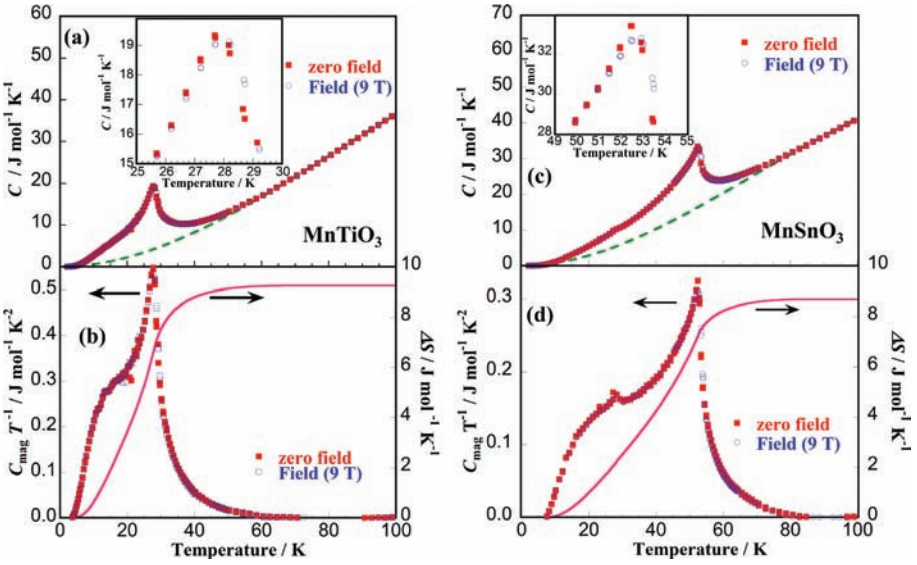

Figure 6. Temperature dependences of the specific heats of $MnTiO_3$ and $MnSnO_3$ under a magnetic field of 0 and 9 T. (a and c) The total specific heats C for $MnTiO_3$ and $MnSnO_3$, respectively. The dashed lines represent the phonon contributions estimated by extrapolation from the data, except for 5 to 60 K for $MnTiO_3$ and 8 to 80 K for $MnSnO_3$. Insets show the C around the peak for $MnTiO_3$ and $MnSnO_3$, respectively. (b and d) Magnetic specific heats divided by temperature $C_{mag}T^{-1}$ for $MnTiO_3$ and $MnSnO_3$, respectively. The solid lines represent the magnetic entropy ΔS.

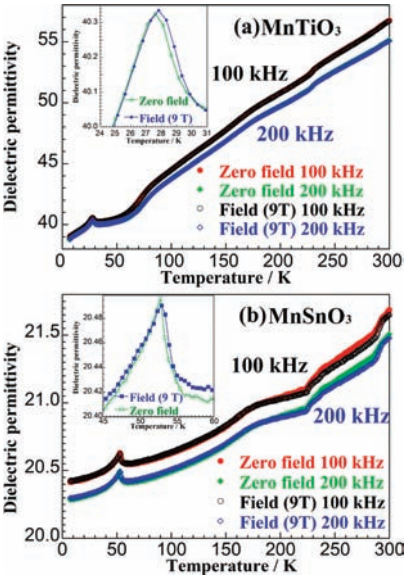

Figure 7. Dielectric permittivity at various frequencies under a magnetic field of 0 and 9 T for $MnTiO_3$ (a) and $MnSnO_3$ (b). Insets show the extended figures for $MnTiO_3$ and $MnSnO_3$, respectively.

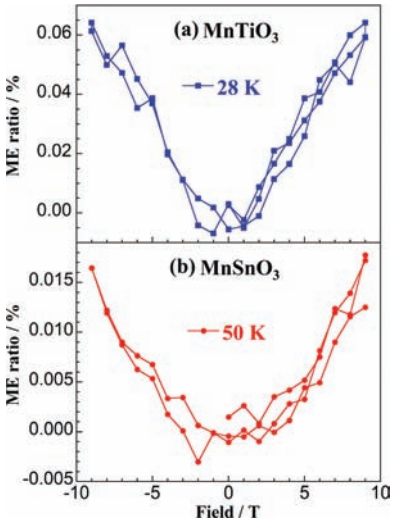

Figure 8. Magnetic field dependences of the ME ratio for an electric field frequency of 100 kHz for $MnTiO_3$ at 28 K (a) and $MnSnO_3$ at 50 K (b).

antiferromagnetic ordering appeared at a higher temperature in $MnSnO_3$.

C. Dielectric Properties of $MnMO_3$ (M = Ti, Sn). The temperature dependences of the dielectric permittivity ε of $MnTiO_3$ and $MnSnO_3$ at two different measurement frequencies of 100 and 200 kHz are shown in Figure 7a,b, respectively. The measurements were performed under a magnetic field of 0 and 9 T. Anomalies were observed in both the compounds at 27.6 and 52.8 K for $MnTiO_3$ and $MnSnO_3$, respectively. These anomalies were independent of the measurement frequencies but shifted slightly to the high temperature side on application of the magnetic field of 9 T, similar to the specific heat anomaly shown in the insets of Figure 6a,c. Comparing Figures 4a and 6a, or Figures 4b and 6b, we see that the anomalies of the dielectric permittivity and the magnetic susceptibility appeared at the same temperature. This behavior indicates the existence of correlation between dielectric and magnetic properties. It is the first time the magnetodielectric coupling in $LiNbO_3$-type compounds is observed. Furthermore, the magnetodielectric ME ratios $(\varepsilon(H) - \varepsilon(0))/\varepsilon(0)$ of $MnTiO_3$ and $MnSnO_3$ were estimated. Here, $\varepsilon(H)$ denotes the dielectric permittivity under a magnetic field of H. Figure 8a,b show the magnetic field dependences of the ME ratio at 28 K for $MnTiO_3$ and 50 K for $MnSnO_3$, respectively. For $MnTiO_3$, the ME response when $H = 9$ T was observed with the largest magnitude being 0.06%. For $MnSnO_3$, the ME response

dx.doi.org/10.1021/ic201006q |*Inorg. Chem.* 2011, 50, 6392–6398

when H = 9 T had a largest magnitude of 0.02%. For reference, the magnetic field dependences of the magnetodielectric ratio for $MnTiO_3$ and $MnSnO_3$ at various temperatures are shown in Figure S1 in the Supporting Information. The observed ME responses for both the compounds were quite less than those for other compounds, e.g., about 560% for perovskite-type $DyMnO_3$ when H = 4 T.[28] In general, ME response diminishes as the difference between ferroelectric ordering and magnetic ordering temperatures increases.[29] $DyMnO_3$ undergoes structural phase transition to the ferroelectric phase accompanying magnetic transition, i.e., ferroelectricity induced by magnetic order resulting in a great ME response. On the other hand, $LiNbO_3$-type $MnMO_3$ is polar even at room temperature, and no structural phase transition is undergone at the magnetic transition. The anomaly in dielectric permittivity is unlikely to be dominated by the change of the ferroelectric polarization. It is therefore natural for $LiNbO_3$-type $MnMO_3$ to exhibit a small ME response. The magnetic and electric properties in $LiNbO_3$-type $MnMO_3$ are correlated in a different manner from the $DyMnO_3$. In $LiNbO_3$-type $MnMO_3$, canted ferromagnetic interaction is generated through ferroelectricity, i.e., weak-ferromagnetism induced by polarization.[8,30] In this type of multiferroics, the magnetic moment is controlled by an external electric field through the change of polarization.

The most important characteristic in multiferroic materials is that the switching of magnetization occurs accompanied by a switching of polarization. In this study, we evaluated the ME response from the change in the dielectric permittivity induced by the magnetic field. Fennie predicted that the switching of polarization by an external electric field would induce 180° switching of the magnetization in multiferroic materials with an LN-type structure.[8] The evaluation of the switching of magnetization by an external electric field should be a vital future work.

CONCLUSION

LN-type $MnMO_3$ (M = Ti, Sn) was prepared using a high pressure and temperature solid-state reaction technique. Both the compounds were crystallized in a polar crystal class. $MnTiO_3$ exhibits greater distortion of oxygen octahedra MO_6 than $MnSnO_3$. This structural feature was attributed to the SOJT active cation, Ti^{4+}. Both of the compounds underwent antiferromagnetic ordering with weak ferromagnetism. Clear anomalies were observed in the dielectric permittivity and specific heat at the onset temperature of weak ferromagnetism for both the compounds, indicating the correlation between magnetic and dielectric properties. This is the first observation of this type in LN-type compounds. These results indicate that LN-type compounds, including 3d transition metals, are suitable candidates for multiferroics, and we believe that our findings could provide a new option for studies on multiferroics.

ASSOCIATED CONTENT

Supporting Information. Magnetic field dependences of magnetodielectric ratio for $MnTiO_3$ and $MnSnO_3$ at various temperatures. This material is available free of charge via the Internet at http://pubs.acs.org.

AUTHOR INFORMATION

Corresponding Author
*E-mail: yoshiyuki.inaguma@gakushuin.ac.jp.

ACKNOWLEDGMENT

The synchrotron XRD measurements were carried out under the Priority Nanotechnology Support Program administered by the Japan Synchrotron Radiation Research Institute (JASRI; Proposal No. 2010A1669). This work was supported by a Grant-in-Aid for Science Research (No. 21360325) of the Japan Society for the Promotion of Science, and a promotional project for the Development of Strategic Research base for private universities, and a matching fund subsidy from the Ministry of Education, Culture, Sports, Science and Technology, Japan.

REFERENCES

(1) Wang, J.; Neaton, J. B.; Zheng, H.; Nagarajan, V.; Ogale, S. B.; Liu, B.; Viehland, D.; Vaithyanathan, V.; Schlom, D. G.; Waghmare, U. V.; Spaldin, N. A.; Rabe, K. M.; Wuttig, M.; Ramesh, R. *Science* **2003**, *299*, 1719–1722.
(2) Kimura, T.; Kawamoto, S.; Yamada, I.; Azuma, M.; Takano, M.; Tokura, Y. *Phys. Rev. B* **2003**, *67*, 180401.
(3) Belik, A. A.; Kamba, S.; Savinov, M.; Nuzhnyy, D.; Tachibana, M.; Takayama-Muromachi, E.; Goian, V. *Phys. Rev. B* **2009**, *79*, 054411.
(4) Smolenskii, G. A.; Chupis, I. E. *Sov. Phys. Usp.* **1982**, *25*, 475–493.
(5) Smolenskii, G. A.; Bokov, V. A. *J. Appl. Phys.* **1964**, *35*, 915–918.
(6) Inaguma, Y.; Yoshida, M.; Katsumata, T. *J. Am. Chem. Soc.* **2008**, *130*, 6704–6705.
(7) Son, J. Y.; Lee, G.; Jo, M. H.; Kim, H.; Jang, H. M.; Shin, Y. H. *J. Am. Chem. Soc.* **2009**, *131*, 8386–8387.
(8) Fennie, C. J. *Phys. Rev. Lett.* **2008**, *100*, 4.
(9) Ok, K. M.; Chi, E. O.; Halasyamani, P. S. *Chem. Soc. Rev.* **2006**, *35*, 710–717.
(10) Leinenweber, K.; Linton, J.; Navrotsky, A.; Fei, Y.; Parise, J. B. *Phys. Chem. Miner.* **1995**, *22*, 251–258.
(11) Hattori, T.; Matsuda, T.; Tsuchiya, T.; Nagai, T.; Yamanaka, T. *Phys. Chem. Miner.* **1999**, *26*, 212–216.
(12) Linton, J. A.; Fei, Y. W.; Navrotsky, A. *Am. Mineral.* **1997**, *82*, 639–642.
(13) Akaogi, M.; Kojitani, H.; Yusa, H.; Yamamoto, R.; Kido, M.; Koyama, K. *Phys. Chem. Minerals* **2005**, *32*, 603–613.
(14) Syono, Y.; Akimoto, S.; Ishikawa, Y.; Endoh, Y. *J. Phys. Chem. Solids* **1969**, *30*, 1665–1672.
(15) Syono, Y.; Sawamoto, H.; Akimoto, S. *Solid State Commun.* **1969**, *7*, 713–716.
(16) Sleight, A. W.; Prewitt, C. T. *Mater. Res. Bul.* **1970**, *5*, 207–212.
(17) Varga, T.; Kumar, A.; Vlahos, E.; Denev, S.; Park, M.; Hong, S.; Sanehira, T.; Wang, Y.; Fennie, C. J.; Streiffer, S. K.; Ke, X.; Schiffer, P.; Gopalan, V.; Mitchell, J. F. *Phys. Rev. Lett.* **2009**, *103*, 047601.
(18) Ko, J. D.; Prewitt, C. T. *Phys. Chem. Minerals* **1988**, *15*, 355–362.
(19) Durand, B.; Loiseleur, H. *J. Appl. Crystallogr.* **1978**, *11*, 156–157.
(20) Izumi, F.; Momma, K. *Solid State Phenom.* **2007**, *130*, 15–20.
(21) Leinenweber, K.; Utsumi, W.; Yoshihiko, T.; Yagi, T.; Kurita, K. *Phys. Chem. Minerals* **1991**, *18*, 244–250.
(22) Momma, K.; Izumi, F. *J. Appl. Crystallogr.* **2008**, *41*, 653–658.
(23) Brown, I. D.; Altermatt, D. *Acta Crystallogr.* **1985**, *B41*, 244–247.
(24) Brown, I. D.; Shannon, R. D. *Acta Crystallogr., Sect. A* **1973**, *A29*, 266–282.
(25) Halasyamani, P. S.; Poeppelmeier, K. R. *Chem. Mater.* **1998**, *10*, 2753–2769.
(26) Kwei, G. H.; Lawson, A. C.; Billinge, S. J. L.; Cheong, S. W. *J. Phys. Chem.* **1993**, *97*, 2368–2377.
(27) Na, C. W.; Han, D. S.; Park, J.; Jo, Y.; Jung, M.-H. *Chem. Commun.* **2006**, 2251–2253.
(28) Goto, T.; Kimura, T.; Lawes, G.; Ramirez, A. P.; Tokura, Y. *Phys. Rev. Lett.* **2004**, *92*, 257201.

(29) Huang, Z. J.; Cao, Y.; Sun, Y. Y.; Xue, Y. Y.; Chu, C. W. *Phys. Rev. B* **1997**, *56*, 2623–2626.
(30) Moriya, T. *Phys. Rev.* **1960**, *120*, 91–98.

■ NOTE ADDED AFTER ASAP PUBLICATION

This paper was published on the Web on June 6, 2011, with the citation for ref 21 missing. The corrected version was reposted on June 10, 2011.